

# Chirality-Memory Molecule: Crystallographic and Spectroscopic Studies on Dynamic Molecular Recognition Events by Fully Substituted Chiral Porphyrins

Yukitami Mizuno,<sup>‡</sup> Takuzo Aida,<sup>\*,‡</sup> and Kentaro Yamaguchi<sup>†,§</sup>

Contribution from the Department of Chemistry and Biotechnology, Graduate School of Engineering, The University of Tokyo, 7-3-1 Hongo, Bunkyo-ku, Tokyo 113-8656, Japan, and Chemical Analysis Center, Chiba University, 1-33 Yayoi-cho, Inage-ku, Chiba 263-8522, Japan

Received January 3, 2000

**Abstract:** X-ray crystallography of a mandelate complex of a  $D_2$ -symmetric saddle-shaped porphyrin such as 2,3,7,8,12,13,17,18-octamethyl-5,15-bis(2',6'-dimethoxyphenyl)-10,20-diphenylporphyrin (**2**) showed that two mandelate anions are hydrogen bonded to the pyrrole NH moieties in a monodentate fashion, where the absolute structure of the porphyrin macrocycle is determined in such a way that the least hindered section of the host molecule accommodates the phenyl group of the mandelate. IR and  $^1\text{H}$  NOESY NMR spectroscopies in  $\text{CH}_2\text{-Cl}_2$  indicated that a similar binding mode is operative in solution. A series of fully substituted chiral porphyrins having different numbers of *o*-dimethoxyphenyl groups at the *meso*-positions (**1–3**) showed different chiral transfer efficiencies and ring inversion activities. Thermal racemization profiles of protonated **2** in a variety of achiral carboxylic acids indicated that the ring inversion rate is dependent on the steric factor as well as the acidity of the carboxylic acid solvent.

## Introduction

Chiral recognition of asymmetric compounds is one of the important subjects not only in the field of supramolecular chemistry but also for medicinal and biomedical applications. In particular, supramolecular approaches to rapid sensing of the absolute configurations of asymmetric compounds have become of increasing interest.<sup>1</sup> From this point of view, novel chromophoric host molecules have recently been developed, which can sense and *memorize* chiral guest configurations via induced-fit interactions.<sup>1d,i–k</sup> We have reported the first example of such chirality-sensing molecules on the basis of a fully substituted chiral porphyrin.<sup>1d</sup> Smith and co-workers have reported that fully substituted porphyrins such as octaalkyltetraarylporphyrins are saddle-shaped due to the steric repulsion among the neighboring substituents on the porphyrin periphery.<sup>2</sup> Thus, porphyrin **2** having two different aryl groups at the adjacent *meso*-positions is chiral with a symmetry group  $D_2$ .<sup>1d</sup> However, the enantiomers of **2** are hardly separable due to its rapid saddle-to-saddle macrocyclic inversion (racemization). On the other hand, we have found that **2** forms a hydrogen-bonded complex with two molecules of a chiral carboxylic acid such as mandelic acid (**4**

in Table 1), in which one of the two possible diastereoisomers is predominantly formed as the result of an induced-fit macrocyclic inversion of the saddle conformation (Scheme 1). Furthermore, even after the chiral guest is replaced by an achiral carboxylic acid such as acetic acid, **2** can retain its optical activity over a long period of time at room temperature. Thus, **2** is a conceptually new chirality sensor that can *memorize* chiral acid configurations.

In the present paper, we report X-ray crystal structure of the mandelate complex of **2**, spectral profiles of the complex in solution, and efficiencies of chirality transfer and memory events with a series of fully substituted chiral porphyrins (**1–3**), and we discuss possible factors affecting this particular dynamic molecular recognition process.

## Results and Discussion

**X-ray Crystallography of the Mandelate Complex of 2.** When an ethyl acetate solution of a mixture of porphyrin (**2**) and racemic mandelic acid (1:2.1) was once heated at 80 °C and allowed to stand at room temperature for 2 days, a crystalline mandelate complex of **2** in the form of a dark greenish blue prism, appropriate for X-ray crystallography, formed. Figure 1 shows an ORTEP view of the complex, in which the porphyrin macrocycle clearly adopts a saddle conformation with the four pyrrole units pointing up and down alternately with respect to the least-squares plane of the

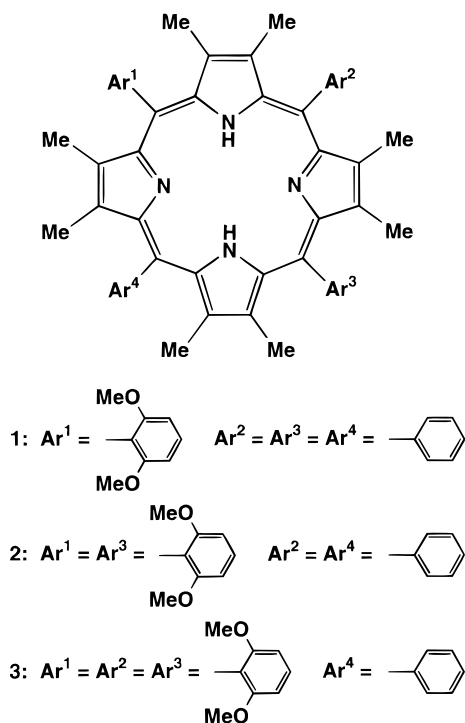
(2) (a) Barkigia, K. M.; Berber, M. D.; Fajer, J.; Medforth, C. J.; Renner, M. W.; Smith, K. M. *J. Am. Chem. Soc.* **1990**, *112*, 8851. (b) Medforth, C. J.; Berber, M. D.; Smith, K. M.; Shelnut, J. A. *Tetrahedron Lett.* **1990**, *31*, 3719. (c) Senge, M. O.; Forsyth, T. P.; Nguyen, L. T.; Smith, K. M. *Angew. Chem., Int. Ed. Engl.* **1994**, *33*, 2485. (d) Medforth, C. J.; Hobbs, J. D.; Rodriguez, M. R.; Abraham, R. J.; Smith, K. M.; Shelnut, J. A. *Inorg. Chem.* **1995**, *34*, 1333. (e) Barkigia, K. M.; Fajer, J.; Berber, M. D.; Smith, K. M. *Acta Crystallogr. Sect. C* **1995**, *C51*, 511. (f) Nurco, D. J.; Medforth, C. J.; Forsyth, T. P.; Olmstead, M. M.; Smith, K. M. *J. Am. Chem. Soc.* **1996**, *118*, 10918.

<sup>‡</sup> The University of Tokyo.

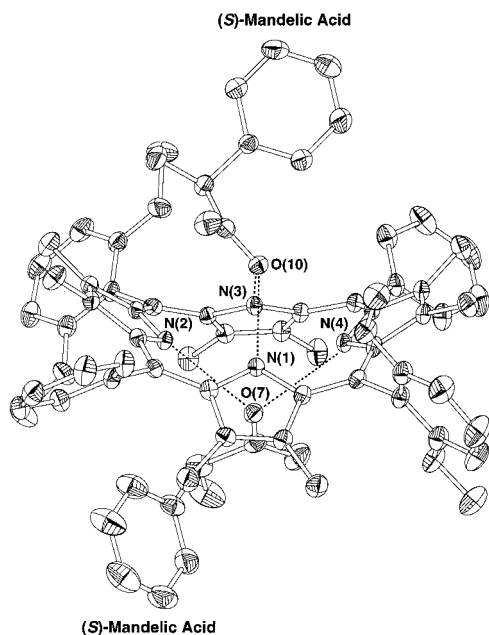
<sup>†</sup> Responsible for X-ray crystallography.

<sup>§</sup> Chiba University.

(1) (a) James, T. D.; Samankumara Sandanayake, K. R. A.; Shinkai, S. *Nature* **1995**, *374*, 345. (b) Kubo, Y.; Maeda, S.; Tokita, S.; Kubo, M. *Nature* **1996**, *382*, 522. (c) Takeuchi, M.; Imada, T.; Shinkai, S. *J. Am. Chem. Soc.* **1996**, *118*, 10658. (d) Furusho, Y.; Kimura, T.; Mizuno, Y.; Aida, T. *J. Am. Chem. Soc.* **1997**, *119*, 5267. (e) Yashima, E.; Matsushima, T.; Okamoto, Y. *J. Am. Chem. Soc.* **1997**, *119*, 6345. (f) Mizutani, T.; Kurahashi, T.; Murakami, T.; Matsumi, N.; Ogoshi, H. *J. Am. Chem. Soc.* **1997**, *119*, 8991. (g) Huang, X.; Rickman, H. B.; Borhan, B.; Berova, N.; Nakanishi, N. *J. Am. Chem. Soc.* **1998**, *120*, 6185. (h) Takeuchi, M.; Imada, T.; Shinkai, S. *Angew. Chem., Int. Ed. Engl.* **1998**, *37*, 2096. (i) Mizuno, T.; Takeuchi, M.; Hamachi, I.; Nakashima, K.; Shinkai, S. *J. Chem. Soc., Perkin Trans. 2* **1998**, 2281. (j) Yashima, E.; Maeda, K.; Okamoto, Y. *Nature* **1999**, *399*, 449. (k) Sugasaki, A.; Ikeda, M.; Takeuchi, M.; Robertson, A.; Shinkai, S. *J. Chem. Soc., Perkin Trans. 1* **1999**, 3259.

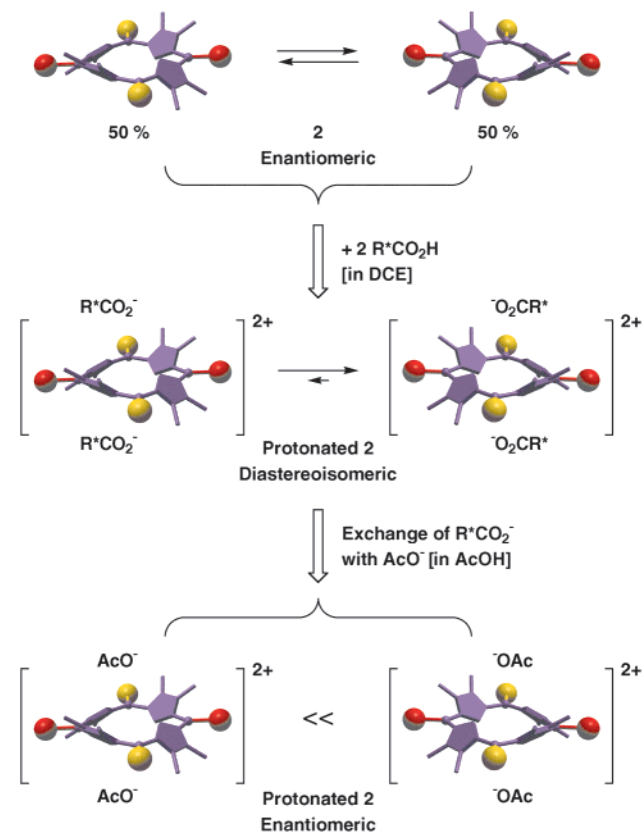


porphyrin. Furthermore, absolute configurations of the mandelate groups on both sides of the porphyrin are identical with each other (*S*-configuration in Figure 1). The crystal structure also shows that the mandelate groups are hydrogen bonded in a monodentate fashion to the pyrrole units, where one oxygen atom of the carboxylate moiety is bonded to two opposing NH functionalities on the same side of the porphyrin, while the other is hydrogen bonded intramolecularly to the  $\alpha$ -hydroxyl group of the mandelate. The four hydrogen-bonded nitrogen–oxygen

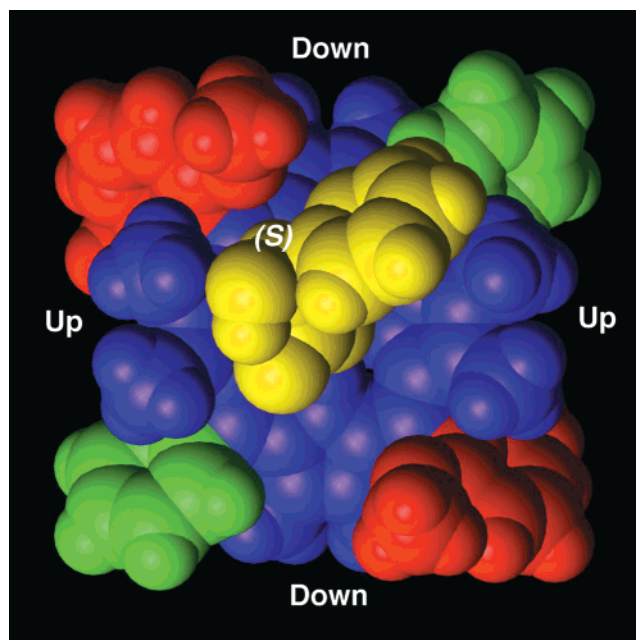


**Figure 1.** ORTEP view of the mandelate complex of **2**. The single crystal was obtained by slow evaporation of an ethyl acetate solution of a mixture of **2** and racemic mandelic acid (1:2.1). The hydrogen atoms are omitted for clarity, and the remaining atoms are represented by Gaussian ellipsoids at the 30% probability level. The asymmetric carbon atoms of the mandelate moieties here both adopt (*S*)-configuration. Selected atom distances ( $\text{\AA}$ ): N(1)–O(10), 2.806(4); N(3)–O(10), 2.792(4); N(2)–O(7), 2.849(4); and N(4)–O(7), 2.827(4).

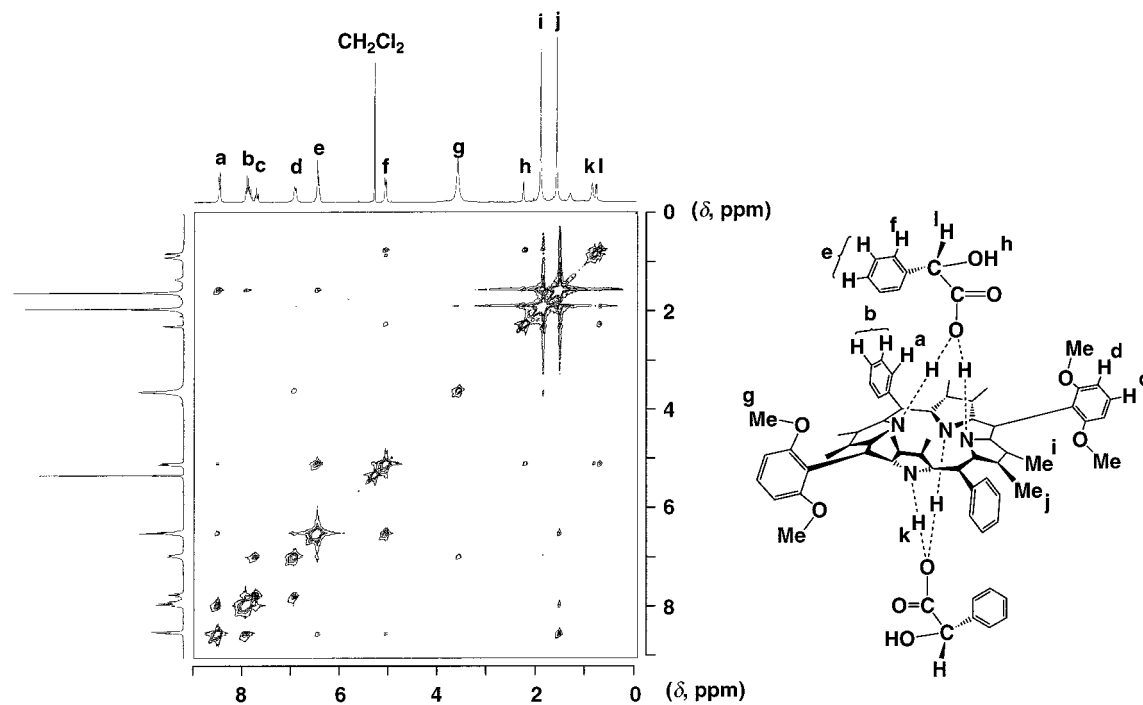
**Scheme 1.** Schematic Representation of Chirality Transfer and Memory Events with Saddle-Shaped Chiral Porphyrin



atom distances are almost identical with one another. This binding mode is in contrast with those reported for the crystal structures of the acetate complexes of saddle-shaped porphyrins, in which the acetate groups are hydrogen bonded in a bidentate fashion to the porphyrin NH.<sup>2c,2e</sup> Figure 2 shows a graphical representation of the top view of the complex, in which the phenyl group of the mandelate is orientated toward the least



**Figure 2.** Graphical representation of a top view of the mandelate complex of **2** (Ph; green, *o*-(MeO)<sub>2</sub>Ar; red, (*S*)-mandelate; yellow). The image was created based on the atomic coordinates of the crystal structure in Figure 1.



**Figure 3.** <sup>1</sup>H NOESY NMR spectrum (600 ms mixing time) in CD<sub>2</sub>Cl<sub>2</sub> at −90 °C of the (*S*)-mandelate complex of **2**, obtained by recrystallization in ethyl acetate. For assignment of the signals, see ref 1d.

hindered section of the host molecule bearing a nonsubstituted *meso*-phenyl group. On the other hand, the  $\alpha$ -hydroxyl group of the mandelate, hydrogen bonded to the carboxylate C–O functionality, is pointing toward the tilted-up pyrrole unit, and the hydrogen atom attached to the asymmetric center of the guest is oriented toward the most hindered section of the host molecule having an *o*-dimethoxyphenyl group. Thus, the chirality transfer from mandelic acid to **2** is realized by the steric interactions of the hydrogen-bonded guest molecule with an asymmetric recognition site (pocket) consisting of two pyrrole units and two *meso*-aryl groups. The recognition site with a clockwise arrangement of tilted-up pyrrole, *o*-dimethoxyphenyl, tilted-down pyrrole, and then nonsubstituted phenyl groups (Figure 2) prefers (*S*)-mandelic acid, while that with the counterclockwise arrangement has an opposite preference for the guest configuration. When the host porphyrin accidentally interacts with mandelic acid of an unfavorable configuration, it can simply flip the saddle conformation to invert the steric preference (induced-fit interaction).

**Spectral Profiles of the Mandelate Complex of 2 in Solution.** Infrared spectroscopy is informative for the mode of carboxylate anion binding. In general, carboxylate ligands coordinated to metal ions in a bidentate fashion exhibit asymmetric and symmetric C–O vibrational frequencies which are  $\sim 150\text{ cm}^{-1}$  apart from each other, while the difference in these two vibrational frequencies for monodentate coordination is much larger.<sup>3</sup> In fact, a KBr pellet sample of the mandelate complex, obtained from **2** and racemic mandelic acid by recrystallization in ethyl acetate, displayed asymmetric and symmetric C–O vibrational frequencies respectively at 1593 and 1354  $\text{cm}^{-1}$ ,<sup>4</sup> whose difference (239  $\text{cm}^{-1}$ ) is much larger than the case of bidentate coordination. On the other hand, the infrared spectrum of the complex in CH<sub>2</sub>Cl<sub>2</sub> was virtually the

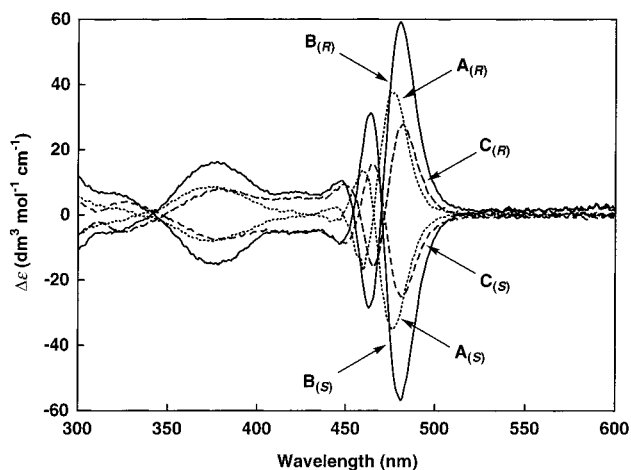
same as that of the solid-state sample, giving a frequency difference of 243  $\text{cm}^{-1}$  between the asymmetric and symmetric C–O vibrations (1595 and 1352  $\text{cm}^{-1}$ , respectively).<sup>4</sup> Therefore, similarly to the case of the crystalline state, the mandelate anions in solution are most likely hydrogen bonded in a monodentate fashion to the pyrrole NH moieties of the porphyrin.

As reported previously, the mandelate complex of **2** has been well characterized by <sup>1</sup>H NMR.<sup>1d</sup> For example, the (*S*)-mandelate complex of **2** in CDCl<sub>3</sub> at −50 °C showed virtually a single MeO signal at  $\delta$  3.65 ppm due to the *o*-dimethoxyphenyl group at the *meso*-position with a negligibly small MeO signal at  $\delta$  3.85 ppm. The intensity ratio of these two signals was  $>99: <1$ , indicating a diastereoisomeric excess higher than 98%. To obtain geometric information in solution, the <sup>1</sup>H NOESY NMR spectrum of the complex was taken in CD<sub>2</sub>Cl<sub>2</sub> at −90 °C. As shown in Figure 3, the spectrum displayed NOE cross-peaks between the phenyl protons (e and f) of the mandelate and the *ortho*-protons (a) of the nonsubstituted phenyl groups at the *meso*-positions of the porphyrin, whereas no such NOE cross-peaks were observed between the guest phenyl protons and the host methoxy protons (g). NOE cross-peaks were also observed between the *meta*-/*para*-protons (e) of the guest phenyl group and the pyrrole- $\beta$ -methyl protons (j) close to the nonsubstituted phenyl groups of the host molecule. These observations indicate that the mandelate complex of **2** in solution adopts a geometrical structure similar to that in the crystalline state.

**Structural Effects on Chirality Transfer and Memory Events.** Porphyrins **1** and **3** with a symmetry group  $C_2$  are also chiral when they adopt a saddle conformation. In fact, (*R*)- and (*S*)-mandelate complexes of **1** and **3** in CHCl<sub>3</sub> showed characteristic CD bands at the visible absorption bands of the porphyrins. Furthermore, similarly to **2**, these porphyrins remained optically active even after the mandelate complexes (diastereoisomeric) were converted into the corresponding acetate complexes (enantiomeric) when dissolved in acetic acid (Figure 4).<sup>1d</sup> Although the CD spectral patterns of optically

(3) (a) Buchler, J. W. In *Porphyrin and Metalloporphyrins*; Smith, K. M., Ed.; Elsevier: Amsterdam, 1975; p 222. (b) Deacon, G. B.; Philips, R. *J. Coord. Chem. Rev.* **1980**, *33*, 227.

(4) See Supporting Information.

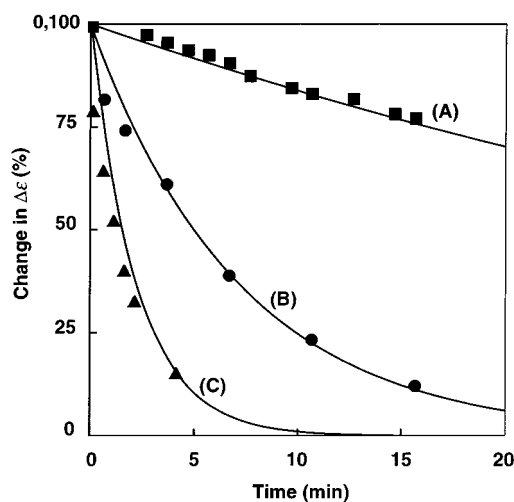


**Figure 4.** Circular dichroism (CD) spectra in acetic acid at 23 °C of the protonated forms of **1** ( $A_{(R)}$ ,  $A_{(S)}$ ), **2** ( $B_{(R)}$ ,  $B_{(S)}$ ), and **3** ( $C_{(R)}$ ,  $C_{(S)}$ ), derived from the (*R*)- and (*S*)-mandelate complexes obtained by recrystallization in ethyl acetate.

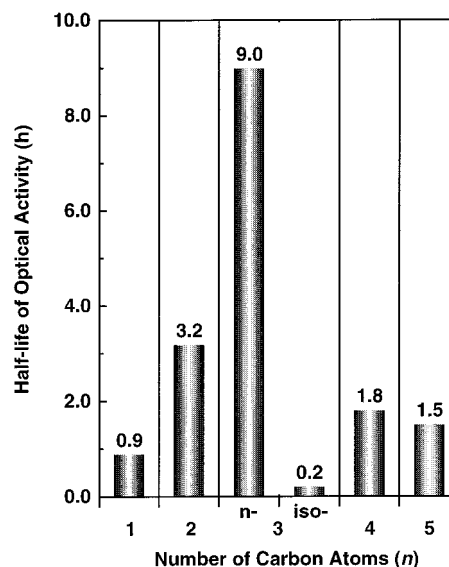
active **1** (Figure 4A) and **3** (Figure 4C) were similar to that of **2** (Figure 4B), the intensities of the CD bands were smaller. Accordingly,  $^1\text{H}$  NMR spectra of the (*S*)-mandelate complexes of **1** and **3** clearly showed some characteristic signals due to diastereoisomers. In  $\text{CDCl}_3$  at  $-50$  °C, the (*S*)-mandelate complex of **1** showed two MeO signals at  $\delta$  3.78 and 3.88 ppm due to the *o*-dimethoxyphenyl group at the *meso*-position with an intensity ratio of 22:77,<sup>4</sup> from which the diastereoisomeric excess was evaluated to be 55%. Similarly, the (*S*)-mandelate complex of **3**, under the same conditions, showed two signals at  $\delta$  8.62 and 8.19 ppm assignable to the *ortho*-protons of the nonsubstituted *meso*-phenyl group with an intensity ratio of 87:13,<sup>4</sup> which corresponds to the diastereoisomeric excess of 74%. From the crystal structure of the mandelate complex of **2** (Figure 2), the lower efficiencies of the chirality transfer, as observed for **1** and **3** having three identical *meso*-aryl groups, are considered reasonable, since the chiral recognition of mandelate anion requires two adjacent *meso*-aryl groups of different steric bulk.

Of further interest is the fact that the lifetimes of the chirality memory of **1–3** in acetic acid were considerably different from one another. For example, when the crystals of the (*S*)-mandelate complex of **2** were dissolved in acetic acid at 74 °C, the optical activity of **2** in the protonated form was decreased with a half-life of 5 min (Figure 5B). On the other hand, the optical activity of protonated **1**, under the same conditions, lasted for a longer period of time (half-life, 39 min; Figure 5A) than that of protonated **2**. In contrast, protonated **3** showed the shortest half-life of the optical activity (1.5 min; Figure 5C) among the three porphyrins examined. The observed thermal racemization is due to the macrocyclic inversion of the saddle conformation. From the thermal racemization profiles, the activation free energies at 298 K ( $\Delta G^\ddagger_{298}$ ) for the macrocyclic inversion of protonated **1–3** in acetic acid were evaluated to be 28.0, 26.1, and 24.4 kcal mol<sup>-1</sup>, respectively.<sup>5</sup> Thus, the *ortho*-substituents on the *meso*-aryl groups of the porphyrin appear to affect the macrocyclic inversion process of the saddle conformation.

In relation to this trend, the inversion rate of the saddle conformation was found to depend also on the acidity and steric bulk of the carboxylic acid solvent. In highly acidic solvents such as dichloroacetic acid ( $\text{p}K_a$  at 25 °C = 1.30) and propiolic



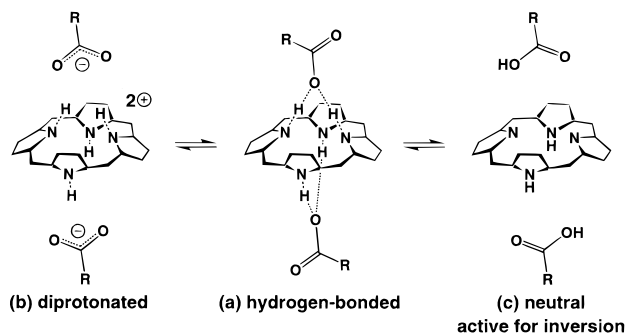
**Figure 5.** Thermal racemization profiles in acetic acid at 74 °C of the protonated forms of **1–3**, derived from the (*S*)-mandelate complexes obtained by recrystallization in ethyl acetate. Changes in  $\Delta\epsilon$  at 478 nm for **1** (A) and 482 nm for **2** (B) and **3** (C).



**Figure 6.** Half-lives of the optical activity of the protonated form of **2** (derived from the (*S*)-mandelate complex obtained by recrystallization in ethyl acetate) in carboxylic acids  $\text{H}(\text{CH}_2)_n\text{CO}_2\text{H}$ , ( $n = 1–5$ ) and  $(\text{CH}_3)_2\text{CHCO}_2\text{H}$  at 57 °C.  $\text{p}K_a$  values of the acids are 4.76 ( $n = 1$ ), 4.87 ( $n = 2$ ), 4.82 ( $n = 3$ ), 4.84 ( $n = 4$ ), 4.88 ( $n = 5$ ), and 4.79 ( $(\text{CH}_3)_2\text{CHCO}_2\text{H}$ ) at 25 °C.<sup>8</sup>

acid ( $\text{HC}\equiv\text{CCO}_2\text{H}$ ; 1.84), the half-lives at 57 °C of the optical activity of protonated **2** were 770 and 820 min, respectively, which are more than 1 order of magnitude longer than that in acetic acid (53 min,  $\text{p}K_a$  at 25 °C = 4.76) under the same conditions. Along this line, the racemization profile of protonated **2** was also investigated in carboxylic acids with different hydrocarbon chains ( $\text{H}(\text{CH}_2)_n\text{CO}_2\text{H}$ ,  $n = 1–5$ ) at 57 °C. Interestingly, the half-life of the optical activity clearly showed a bell-shaped dependency on the hydrocarbon chain length of  $\text{H}(\text{CH}_2)_n\text{CO}_2\text{H}$ , although the  $\text{p}K_a$  values of these acids are all in the range 4.7–4.9 (Figure 6). In particular, the slowest racemization was observed in *n*-butyric acid ( $n = 3$ ,  $\text{p}K_a = 4.82$ ), where the half-life of the optical activity (540 min) was almost 1 order of magnitude longer than that in acetic acid. On the other hand, when isobutyric acid ( $\text{p}K_a = 4.79$ ) was used as a solvent in place of *n*-butyric acid, the half-life of the optical

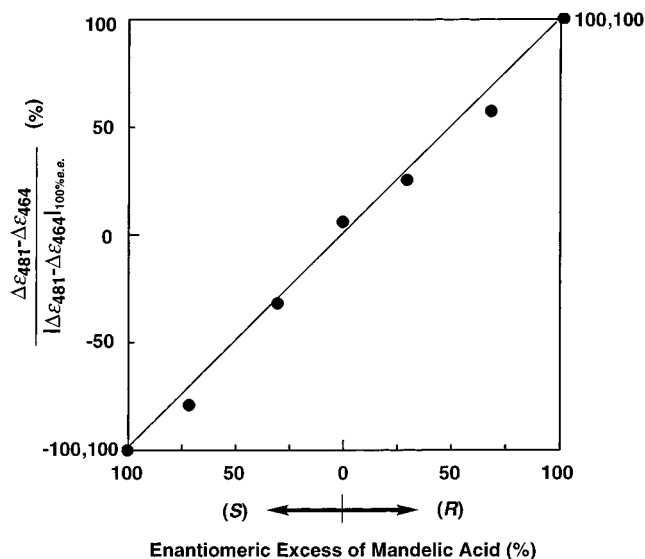
(5) For activation free energies of the macrocyclic inversion of octaethyltetraphenylporphyrin free base and metal complexes in pyridine, see ref 2a.

**Scheme 2.** A Possible Equilibrium for Saddle-Shaped Porphyrins in Carboxylic Acid

activity was short (11 min). In carboxylic acids, there should be at least three different porphyrin species, i.e., protonated and complexed porphyrin (a), protonated but uncomplexed porphyrin (b), and nonprotonated and uncomplexed porphyrin (c) (Scheme 2), where neutral species (c) most likely undergoes thermal-induced racemization (macrocyclic inversion) via a planar transition state. In contrast, species (b) in a diprotonated form is highly reluctant to racemization, since the planar transition state is energetically unfavorable due to an electrostatic repulsion among the positively charged nitrogen atoms. The racemization of hydrogen-bonded complex (a) is also unlikely, because of a possible locking of the saddle-shaped conformation. In carboxylic acids of low  $pK_a$  values ( $<2$ ) such as dichloroacetic acid and propionic acid, diprotonated species (b) must be predominant. On the other hand, in carboxylic acids with  $pK_a$  of 4.7–4.9, the porphyrin should exist mostly in hydrogen-bonded form (a), where a van der Waals interaction between the saddle-shaped pocket of the porphyrin and the hydrocarbon chain of the acid would stabilize the hydrogen-bonding interaction (*n*-butyric acid). However, in sterically hindered carboxylic acids such as isobutyric acid, hydrogen-bonded species (a) must be energetically unstable and frequently dissociate into neutral species (c), which is active for the macrocyclic inversion.

**Performance of 2 as a Chirality Sensor.** Among saddle-shaped porphyrins 1–3, 2 with the highest chirality-transfer efficiency was chosen, and its performance as chirality sensor was investigated in detail. Upon titration of 2 with (*S*)-mandelic acid in 1,2-dichloroethane (DCE,  $[2] \approx 10^{-4}$  M) at 24 °C, the intensities of the CD bands of protonated 2, measured in acetic acid ( $[2] \approx 10^{-6}$  M), were increased as the mole ratio [mandelic acid]/[2] was higher and finally reached a plateau when the guest/host mole ratio exceeded 2.<sup>4</sup> This result indicates that the two-to-one complexation of mandelic acid with 2 is established even under such dilute conditions. On the other hand, when 2 was mixed with mandelic acid of different optical purities in DCE ( $[2] \approx 10^{-4}$  M, [mandelic acid]/[2] = 2.1), the observed CD intensities in acetic acid for the protonated form of 2 displayed a linear correlation with the enantiomeric excess (ee) of the guest (Figure 7). Thus, the optical purity of mandelic acid can be determined from the intensities of the CD bands of 2.

In addition to mandelic acid, a wide variety of chiral carboxylic acids (Table 1) can be diagnosed by 2,<sup>1d</sup> where the absolute configurations of 5–8 and 10–14 were all predictable, by analogy to the case of mandelic acid (4), from the sign of the CD band of 2 at 482 nm in acetic acid after complexation with the carboxylic acids: The CD sign apparently showed a certain correlation with the relative steric bulk of the two substituents at the asymmetric center other than the hydrogen atom and carboxylic acid functionality. In this sense, acids 9,



**Figure 7.** Circular dichroism (CD) spectral responses of 2 toward mandelic acid of different optical purities. 2 and the acid were mixed at a mole ratio of 1:2.1 in 1,2-dichloroethane, and the solution was poured into acetic acid for CD spectroscopy at 24 °C.  $\Delta\epsilon_{481}$  and  $\Delta\epsilon_{464}$  represent the intensities of the CD bands at 481 and 464 nm, respectively, and  $|\Delta\epsilon_{481} - \Delta\epsilon_{464}|_{100\%ee}$  represents their absolute difference for enantiomerically pure mandelic acid.

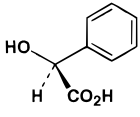
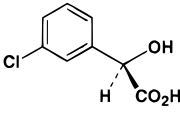
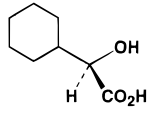
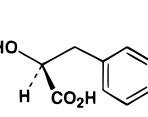
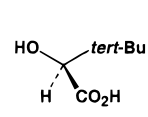
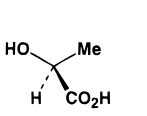
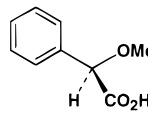
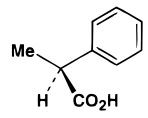
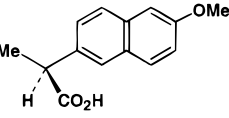
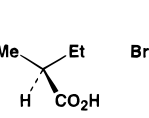
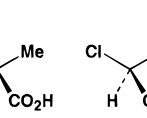

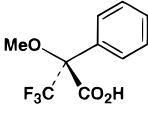
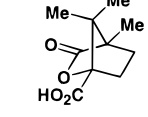
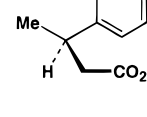
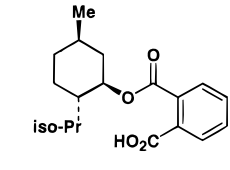
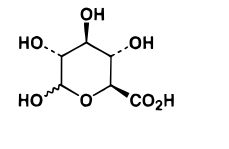
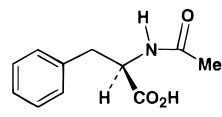
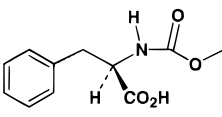
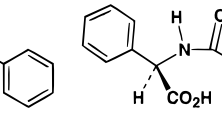
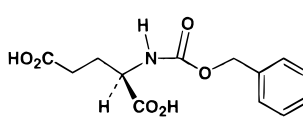
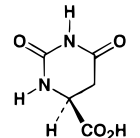
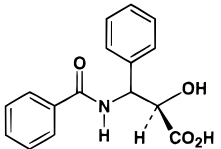
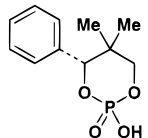
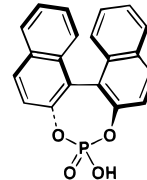
13, and 15 may be located on a borderline for the prediction, since the steric bulks of the corresponding substituents at the chiral center are not much different from each other. 2 can also be applicable to the chirality sensing of acids 16 and 17 having a quaternary asymmetric center. Of further interest, 2 was unable to read out the chirality of acid 18 with a primary carboxylic acid functionality, but the complex of 2 with 19 was CD active although the chiral center of the acid is separated by five bonds from the carboxylic acid residue. 2 can also diagnose the absolute configurations of a sugar derivative such as 20,  $\alpha$ - and  $\beta$ -amino acid derivatives 21–26, and phosphoric acids 27 and 28. It should be emphasized here that saddle-shaped porphyrin 2 as a chirality sensor can take great advantage of not only its enhanced circular dichroism activity in the visible region<sup>6</sup> but also its ability of memorizing the chiral recognition event. This allows us to determine the guest configuration on the basis of the inherent CD profile of 2 without any interfering effects of the guest molecules.

## Conclusion

In the present paper, we succeeded in the first crystallographic determination of the absolute structure of a chiral saddle-shaped porphyrin (2). This achievement allows us to make a direct structural correlation of the absolute conformation of the saddle in solution with its circular dichroism profile. Furthermore, the crystal structure of the complex with mandelic acid, together with the notable structural effects on the chirality transfer and memory events, will also provide a new strategy for the molecular design of chirality sensors that can be applied to a wider variety of chiral substrates. Transfer of structural information in noncovalent systems is one of the challenging subjects in supramolecular chemistry involving dynamic molecular recognition events. Chemical amplification of the transferred

(6) (a) Harada, N.; Nakanishi, K. *Circular Dichroic Spectroscopy—Exciton Coupling in Organic Stereochemistry*; University Science Books: Mill Valley, CA, 1983. (b) Nakanishi, K.; Berova, N. In *Circular Dichroism—Principles and Applications*; Nakanishi, K., Berova, N., Woody, R. W., Eds.; VCH: New York, 1994; pp 361–398.

Table 1. CD Sign at 482 nm of **2** in Acetic Acid after Complexation in Ethyl Acetate/1,2-Dichloroethane

Carboxylic Acids					
					
4 -	5 +	6 +	7 -	8 -	9 -
					
10 +	11 -	12 -	13 -	14 +	15 -
					
16 +	17 -	18 Not Detected	19 +	20 +	
Amino Acid Derivatives					
					
21 +	22 +	23 +			
					
24 +	25 -	26 +			
Phosphoric Acids					
					
27 -	28 -				

information will be a highly interesting subject worthy of further investigation.

### Experimental Section

**Materials.** Dichloromethane ( $\text{CH}_2\text{Cl}_2$ ), 1,2-dichloroethane (DCE), and ethyl acetate (EtOAc) were distilled from  $\text{CaH}_2$  under nitrogen. Ethylene glycol was distilled from  $\text{CaSO}_4$  under reduced pressure. These solvents were stored under nitrogen.  $\text{BF}_3$  etherate and benzaldehyde were distilled under reduced pressure and stored in a nitrogen atmosphere. Carboxylic acids used as solvents for CD measurements

were distilled from molecular sieves 4A (Aldrich) and stored under nitrogen. *p*-Chloranil (Aldrich) was used as received.

**5-Phenyl-2,3,7,8-tetramethylpyrromethane:**<sup>7</sup> To a  $\text{CH}_2\text{Cl}_2$  (5.0 mL) solution of a mixture of ethyl 3,4-dimethyl-2-pyrrolicarboxylate<sup>7a</sup> (508 mg, 3.04 mmol) and benzaldehyde (0.15 mL, 1.4 mmol) was added

(7) (a) Ono, N.; Kawamura, H.; Bougauchi, M.; Maruyama, K. *Tetrahedron* **1990**, *46*, 7483. (b) Wallace, D. M.; Leung, S. H.; Senge, M. O.; Smith, K. M. *J. Org. Chem.* **1993**, *58*, 7245. (c) Lindsey, J. S.; MacCrum, K. A.; Tyhonas, J. S.; Chung, Y. *J. Org. Chem.* **1994**, *59*, 579.

(8) Dean, J. A. *Lange's Handbook of Chemistry*, 13th ed.; McGraw-Hill: New York, 1985; Section 5.

BF<sub>3</sub> etherate (0.02 mL, 0.2 mmol), and the mixture was stirred under nitrogen for 24 h at room temperature. Then, the mixture was shaken with aqueous NaHCO<sub>3</sub> and extracted with CH<sub>2</sub>Cl<sub>2</sub>. The combined extracts were washed with brine, and the organic phase that separated was dried over Na<sub>2</sub>SO<sub>4</sub> and evaporated to dryness, to give diethyl 5-phenyl-2,3,7,8-tetramethylpyrromethane-1,9-dicarboxylate in 84% yield (538 mg). <sup>1</sup>H NMR (270 MHz, CDCl<sub>3</sub>, 25 °C): δ 8.21 (2H, s, NH), 7.34 (3H, m, *m*-*p*-H in C<sub>6</sub>H<sub>5</sub>), 7.11 (2H, d, *J* = 3.5 Hz, *o*-H in C<sub>6</sub>H<sub>5</sub>), 5.51 (1H, s, CH), 4.28 (4H, q, *J* = 7.1 Hz, CO<sub>2</sub>CH<sub>2</sub>Me), 2.24 and 1.83 (12H, s, pyrrole-β-CH<sub>3</sub>), 1.35 (6H, t, *J* = 7.1 Hz, CO<sub>2</sub>-CH<sub>2</sub>CH<sub>3</sub>). FAB-MS calcd for C<sub>21</sub>H<sub>26</sub>N<sub>2</sub>O<sub>2</sub> (M<sup>+</sup>) 422, obsd 422. The dicarboxylate (157 mg, 0.373 mmol) was dissolved in ethylene glycol (6.5 mL) containing NaOH (98 mg, 2.4 mmol), and the solution was refluxed for 0.5 h. Then, the reaction mixture was shaken with CH<sub>2</sub>-Cl<sub>2</sub>/water and extracted with CH<sub>2</sub>Cl<sub>2</sub>. The combined extracts were washed with brine, and the organic phase that separated was dried over Na<sub>2</sub>SO<sub>4</sub> and evaporated to dryness. The residue was dissolved in benzene and freeze-dried to give 5-phenyl-2,3,7,8-tetramethylpyrromethane, quantitatively, as a brown powder. <sup>1</sup>H NMR (270 MHz, CDCl<sub>3</sub>, 25 °C): δ 7.30 (3H, m, *m*-*p*-H in C<sub>6</sub>H<sub>5</sub>), 7.14 (2H, d, *J* = 7.8 Hz, *o*-H in C<sub>6</sub>H<sub>5</sub>), 6.40 (2H, d, *J* = 1.5 Hz, pyrrole-α-H), 5.49 (1H, s, CH), 2.03 and 1.81 (12H, s, pyrrole-β-CH<sub>3</sub>). FAB-MS calcd for C<sub>21</sub>H<sub>26</sub>N<sub>2</sub>O<sub>2</sub> (M<sup>+</sup>) 278, obsd 278.

#### 5-(2',6'-Dimethoxyphenyl)-2,3,7,8-tetramethylpyrromethane<sup>7</sup>

To a CH<sub>2</sub>Cl<sub>2</sub> (15 mL) solution of a mixture of ethyl 3,4-dimethyl-2-pyrrolicarboxylate<sup>7a</sup> (2.63 g, 15.7 mmol) and 2,6-dimethoxybenzaldehyde (1.43 g, 8.62 mmol) was added BF<sub>3</sub> etherate (0.11 mL, 0.87 mmol), and the mixture was stirred under nitrogen for 24 h at room temperature. Then, the reaction mixture was shaken with aqueous NaHCO<sub>3</sub> and extracted with CH<sub>2</sub>Cl<sub>2</sub>. The combined extracts were washed with brine, and the organic phase that separated was dried over Na<sub>2</sub>SO<sub>4</sub> and evaporated to dryness. Then, the residue was subjected to recrystallization from EtOH, to give diethyl 5-(2',6'-dimethoxyphenyl)-2,3,7,8-tetramethylpyrromethane-1,9-dicarboxylate in 88% yield (3.32 g). <sup>1</sup>H NMR (270 MHz, CDCl<sub>3</sub>, 25 °C): δ 9.11 (2H, s, NH), 7.21 (1H, t, *J* = 8.3 Hz, *p*-H in C<sub>6</sub>H<sub>3</sub>(OMe)<sub>2</sub>), 6.63 (2H, d, *J* = 8.3 Hz, *m*-H in C<sub>6</sub>H<sub>3</sub>(OMe)<sub>2</sub>), 6.23 (1H, s, CH), 4.29 (4H, q, *J* = 7.1 Hz, CO<sub>2</sub>CH<sub>2</sub>Me), 3.83 (6H, s, OCH<sub>3</sub>), 2.24 and 1.83 (12H, s, pyrrole-β-CH<sub>3</sub>), 1.35 (6H, t, *J* = 7.1 Hz, CO<sub>2</sub>CH<sub>2</sub>CH<sub>3</sub>). FAB-MS calcd for C<sub>27</sub>H<sub>34</sub>N<sub>2</sub>O<sub>6</sub> (M<sup>+</sup>) 482, obsd 482. Anal. Calcd. for C<sub>27</sub>H<sub>34</sub>N<sub>2</sub>O<sub>6</sub>: C, 67.20; H, 7.10; N, 5.80. Found: C, 67.30; H, 7.02; N, 5.97. The dicarboxylate (425 mg) was dissolved in ethylene glycol (8.0 mL) containing NaOH (189 mg, 4.73 mmol), and the solution was refluxed for 0.5 h. Then, the reaction mixture was shaken with CH<sub>2</sub>Cl<sub>2</sub>/water, and extracted with CH<sub>2</sub>Cl<sub>2</sub>. The combined extracts were washed with brine, and the organic phase that separated was dried over Na<sub>2</sub>SO<sub>4</sub> and evaporated to dryness. Then, the residue was dissolved in benzene and freeze-dried to give 5-(2',6'-dimethoxyphenyl)-2,3,7,8-tetramethylpyrromethane, quantitatively, as a brown powder. <sup>1</sup>H NMR (270 MHz, CDCl<sub>3</sub>, 25 °C): δ 8.26 (2H, s, br, NH), 7.14 (1H, t, *J* = 8.3 Hz, *p*-H in C<sub>6</sub>H<sub>3</sub>), 6.61 (2H, d, *J* = 8.3 Hz, *m*-H in C<sub>6</sub>H<sub>3</sub>), 6.38 (2H, d, *J* = 1.2 Hz, pyrrole-α-H), 6.19 (1H, s, CH), 3.7 (6H, s, OCH<sub>3</sub>), 2.00 and 1.82 (12H, s, pyrrole-β-CH<sub>3</sub>). HRMS calcd for C<sub>21</sub>H<sub>26</sub>N<sub>2</sub>O<sub>2</sub> (M<sup>+</sup>) 338.1994, obsd 338.2010.

**2,3,7,8,12,13,17,18-Octamethyl-5-(2',6'-dimethoxyphenyl)-10,15,20-triphenylporphyrin (1):** To a CH<sub>2</sub>Cl<sub>2</sub> (27 mL) solution of a mixture of benzaldehyde (0.27 mL, 2.7 mmol), 5-(2',6'-dimethoxyphenyl)-2,3,7,8-tetramethylpyrromethane (379 mg, 1.12 mmol), 5-phenyl-2,3,7,8-tetramethylpyrromethane (276 mg, 0.990 mmol), and a dehydrating agent such as molecular sieves 4A (2 g) was added BF<sub>3</sub> etherate (0.035 mL, 0.279 mmol), and the mixture was stirred under nitrogen at room temperature. After 2 h, *p*-chloranil (778 mg, 3.16 mmol) was added to the reaction mixture, and stirring was continued for 2 h. Then, molecular sieves 4A were removed by filtration, and a black filtrate was shaken with aqueous Na<sub>2</sub>S<sub>2</sub>O<sub>3</sub> and extracted with CH<sub>2</sub>Cl<sub>2</sub>. The combined extracts were washed with brine, and the organic phase that separated was dried over Na<sub>2</sub>SO<sub>4</sub> and evaporated to dryness. Then, the residue was chromatographed on alumina with CHCl<sub>3</sub>/hexane (7:3) containing 3% Et<sub>2</sub>NH as eluent, where the second green band was collected and subjected to recrystallization from CH<sub>2</sub>Cl<sub>2</sub>/ethanolic KOH, to give **1** in 7% yield (27.9 mg). UV/vis (AcOH): λ<sub>max</sub>, nm (ε, mol<sup>-1</sup>

dm<sup>3</sup> cm<sup>-1</sup>): 397 (26900), 466 (270500), 627 (8800), 683 (28900). <sup>1</sup>H NMR (270 MHz, CDCl<sub>3</sub>, 25 °C): δ 8.30–8.21 (6H, m, *o*-H in C<sub>6</sub>H<sub>5</sub>), 7.75–7.65 (10H, m, *p*-*p*-H in C<sub>6</sub>H<sub>5</sub> + *p*-H in C<sub>6</sub>H<sub>3</sub>(OMe)<sub>2</sub>), 6.93 (2H, d, *J* = 8.34 Hz, *m*-H in C<sub>6</sub>H<sub>3</sub>(OMe)<sub>2</sub>), 3.76 (6H, s, OCH<sub>3</sub> in C<sub>6</sub>H<sub>3</sub>(OMe)<sub>2</sub>), 2.07 (6H, s, pyrrole-β-CH<sub>3</sub> closest to C<sub>6</sub>H<sub>3</sub>(OMe)<sub>2</sub>), 1.88 (6H, s, pyrrole-β-CH<sub>3</sub> second closest to C<sub>6</sub>H<sub>3</sub>(OMe)<sub>2</sub>), 1.83 (12H, s, pyrrole-β-CH<sub>3</sub> between two Ph groups), -2.43 and -2.54 (2H, s, NH; observable at -90 °C). HRMS calcd for C<sub>54</sub>H<sub>51</sub>N<sub>4</sub>O<sub>2</sub> (M + H<sup>+</sup>) 787.4012, obsd 787.3987.

**2,3,7,8,12,13,17,18-Octamethyl-5,15-bis(2',6'-dimethoxyphenyl)-10,20-diphenylporphyrin (2)<sup>1d</sup> and 2,3,7,8,12,13,17,18-octamethyl-5,10,15-tris(2',6'-dimethoxyphenyl)-20-phenylporphyrin (3):** To a CH<sub>2</sub>Cl<sub>2</sub> (8.0 mL) solution of a mixture of benzaldehyde (0.08 mL, 0.8 mmol), 5-(2',6'-dimethoxyphenyl)-2,3,7,8-tetramethylpyrromethane (219 mg, 0.648 mmol), and a dehydrating agent such as molecular sieves 4A (1 g) was added BF<sub>3</sub> etherate (0.01 mL, 0.08 mmol), and the mixture was stirred under nitrogen at room temperature. After 2 h, *p*-chloranil (244 mg, 0.994 mmol) was added to the reaction mixture, and stirring was continued for 2 h. Then, molecular sieves 4A were removed by filtration, and a black filtrate was shaken with aqueous Na<sub>2</sub>S<sub>2</sub>O<sub>3</sub> and extracted with CH<sub>2</sub>Cl<sub>2</sub>. The combined extracts were washed with brine, and the organic phase that separated was dried over Na<sub>2</sub>SO<sub>4</sub> and evaporated to dryness. Then, the residue was chromatographed on alumina with CHCl<sub>3</sub> containing 0.5% Et<sub>2</sub>NH as eluent, where the first and second green bands were collected and subjected to recrystallization from CH<sub>2</sub>Cl<sub>2</sub>/ethanolic KOH, to give **2** and **3** in 13% (35.8 mg) and 4% (8.1 mg) yield, respectively. **2**: UV/vis (AcOH), λ<sub>max</sub>, nm (ε, mol<sup>-1</sup> dm<sup>3</sup> cm<sup>-1</sup>): 467 (220000), 619 (8300), 680 (21000). <sup>1</sup>H NMR (270 MHz, CDCl<sub>3</sub>, 23 °C): δ 8.21–8.14 (4H, m, *o*-H in C<sub>6</sub>H<sub>5</sub>), 7.70–7.65 (6H, m, *m*-*p*-H in C<sub>6</sub>H<sub>5</sub>), 7.64 (2H, t, *J* = 8.4 Hz, *p*-H in C<sub>6</sub>H<sub>3</sub>(OMe)<sub>2</sub>), 6.93 (4H, d, *J* = 8.4 Hz, *m*-H in C<sub>6</sub>H<sub>3</sub>(OMe)<sub>2</sub>), 3.69 (12H, s, OCH<sub>3</sub> in C<sub>6</sub>H<sub>3</sub>(OMe)<sub>2</sub>), 2.05 (12H, s, pyrrole-β-CH<sub>3</sub> close to C<sub>6</sub>H<sub>3</sub>(OMe)<sub>2</sub>), 1.84 (12H, s, pyrrole-β-CH<sub>3</sub> close to C<sub>6</sub>H<sub>5</sub>), -1.9 (2H, s, NH). HRMS calcd for C<sub>58</sub>H<sub>59</sub>N<sub>4</sub>O<sub>6</sub> (M + H<sup>+</sup>) 847.4223, obsd 847.4279. **3**: UV/vis (AcOH), λ<sub>max</sub>, nm (ε, mol<sup>-1</sup> dm<sup>3</sup> cm<sup>-1</sup>): 385 (24600), 467 (241200), 617 (8800), 674 (20100). <sup>1</sup>H NMR (270 MHz, CDCl<sub>3</sub>, 23 °C): δ 8.20–8.16 (2H, m, *o*-H in C<sub>6</sub>H<sub>5</sub>), 7.71–7.59 (12H, m, *m*-*p*-H in C<sub>6</sub>H<sub>5</sub> + *p*-H in C<sub>6</sub>H<sub>3</sub>(OMe)<sub>2</sub>), 6.93 (4H, d, *J* = 8.3 Hz, *m*-H in 5-/15-C<sub>6</sub>H<sub>3</sub>(OMe)<sub>2</sub>), 6.92 (2H, d, *J* = 8.3 Hz, *m*-H in 10-C<sub>6</sub>H<sub>3</sub>(OMe)<sub>2</sub>), 3.67 (12H, s, OCH<sub>3</sub> in 5-/15-C<sub>6</sub>H<sub>3</sub>(OMe)<sub>2</sub>), 3.63 (6H, s, OCH<sub>3</sub> in 10-C<sub>6</sub>H<sub>3</sub>(OMe)<sub>2</sub>), 2.06 (18H, s, pyrrole-β-CH<sub>3</sub> close to C<sub>6</sub>H<sub>3</sub>(OMe)<sub>2</sub>), 1.85 (6H, s, pyrrole-β-CH<sub>3</sub> close to C<sub>6</sub>H<sub>5</sub>), -2.59 and -2.63 (2H, s, NH; observable at -90 °C). HRMS calcd for C<sub>58</sub>H<sub>59</sub>N<sub>4</sub>O<sub>6</sub> (M + H<sup>+</sup>) 907.4435, obsd 907.4485.

**Measurements.** NMR spectra were measured on a JEOL type GSX-270 spectrometer operating at 270 MHz. UV-visible spectra were recorded on a JASCO type V-560 spectrophotometer. CD spectra were recorded on a JASCO type J-720 spectropolarimeter. IR spectra were recorded in a KBr pellet or CH<sub>2</sub>Cl<sub>2</sub> at 21–23 °C on a JASCO type FT-IR-5300 infrared spectrometer.

**Crystallographic Analysis.** An ethyl acetate (EtOAc) solution of a mixture of **2** (6 mg, 7 mmol) and racemic mandelic acid (2 mg, 14 mmol) was once heated at 80 °C and then allowed to cool to room temperature. The solution was allowed to stand at room temperature in a glass bottle with a porous cap to allow slow evaporation of the solvent, to give in 2 days a crystalline mandelate complex of **2**. X-ray crystallographic analysis was undertaken using a charge coupled device (CCD) diffractometer Bruker SMART 1000 with monochromated Mo Kα radiation (λ = 0.7101 Å) using SAINT (Siemens) for cell refinement and data reduction. Absorption correction was not applied. The crystal structure was solved by using SIR97 and refined on *F* by the full-matrix least-squares method included in TEXSAN ver. 1.1 (Molecular Structure Co.). Non-H atoms were refined anisotropically. All H atoms with isotropic thermal parameters were located on the calculated positions (not refined). Crystal and experimental data: dark greenish blue prism (0.45 × 0.40 × 0.35 mm), C<sub>56</sub>H<sub>56</sub>N<sub>4</sub>O<sub>4</sub>·2C<sub>6</sub>H<sub>7</sub>O<sub>3</sub>·2C<sub>4</sub>H<sub>8</sub>O<sub>2</sub>·3H<sub>2</sub>O (two ethyl acetate and three water molecules were included in an asymmetric unit), triclinic *P*1̄, *a* = 13.888(2) Å, *b* = 15.866(2) Å, *c* = 17.869(2) Å, α = 77.632(2)°, β = 73.910(2)°, γ = 77.116(2)°, *V* = 3638.7(6) Å<sup>3</sup>, *Z* = 2, *D*<sub>calcd</sub> = 1.261 g·cm<sup>-3</sup>, *F*<sub>000</sub> = 1472, μ(Mo Kα) = 0.88 cm<sup>-1</sup>; *T* = -100 °C, 2θ<sub>max</sub> = 57.0°, scans, 21970

reflections measured, 16015 unique, 6975 with  $I > 3.0\sigma(I)$ , 911 variables,  $R = 0.066$ ,  $R_w = 0.086$ ,  $S = 1.97$ ,  $(\Delta/\sigma)_{\max} = 0.25$ ,  $\rho_{\max} = 0.47 \text{ e}^-/\text{\AA}$ ,  $\rho_{\min} = -0.41 \text{ e}^-/\text{\AA}$ . The ORTEP view was drawn by CAChe (Oxford Molecular Ltd.).

**Acknowledgment.** Y.M. thanks the JSPS Research Fellowship for Young Scientists.

**Supporting Information Available:** Numbering scheme (Nos. 1, 2), tables of atomic coordinates and isotropic displacement parameters (No. 3), anisotropic displacement parameters (No. 4), bond lengths (No. 5), angles (No. 6), torsion angles

(No. 7) for final positional parameters for the crystalline ( $\pm$ )-mandelate complex of **2** (an X-ray crystallographic file, in CIF format), IR spectra ( $1800\text{--}1200 \text{ cm}^{-1}$ ) of a KBr pellet sample and a  $\text{CH}_2\text{Cl}_2$  solution of the ( $\pm$ )-mandelate complex of **2** (No. 8),  $^1\text{H}$  NMR spectra ( $\text{CDCl}_3$ ,  $-50 \text{ }^\circ\text{C}$ ) of the (*S*)-mandelate complexes of **1** and **3** (Nos. 9, 10), and results of CD titration of **2** with (*S*)-mandelic acid (No. 11) (PDF). This material is available free of charge via the Internet at <http://pubs.acs.org>.

JA000052O